Applied Thermal Engineering 98 (2016) 568–574

Contents lists available at ScienceDirect

Applied Thermal Engineering

journal homepage: www.elsevier.com/locate/apthermeng

Research Paper

Effects of different adsorber bed designs on in-situ water uptake rate measurements of AQSOA FAM-Z02 for vehicle air conditioning applications

Amir Sharafian [1], Seyyed Mahdi Nemati Mehr [1], Wendell Huttema, Majid Bahrami *

Laboratory for Alternative Energy Conversion (LAEC), School of Mechatronic Systems Engineering, Simon Fraser University, BC, V3T 0A3 Canada

HIGHLIGHTS

- Water uptake rate of AQSOA FAM-Z02 packed in an adsorber bed is measured in-situ.
- Effects of two different adsorber bed designs are studied on water uptake rate.
- High heat transfer surface area and small fin spacing are key features of a well-designed adsorber bed.
- Specific cooling power of 112.9 W/kg is achieved by in-situ water uptake rate measurements of AQSOA FAM-Z02.

ARTICLE INFO

Article history:
Received 5 July 2015
Accepted 10 December 2015
Available online 8 January 2016

Keywords:
AQSOA FAM-Z02
Uptake rate
Adsorption cooling system
Air conditioning

ABSTRACT

Adsorption cooling systems (ACS) utilize waste heat to produce the cooling power required for air conditioning (A/C) in vehicles. In addition to having an adsorbent with high adsorbate uptake rate and thermal conductivity, different adsorber bed designs can significantly affect the performance of an ACS. In this study, the water uptake rate of AQSOA FAM-Z02 packed in two different adsorber beds is measured in-situ under adsorption and desorption temperatures of 30 and 90 °C, and the water vapor supplied at 20 °C. The effects of some parameters, such as changes in the density of heat transfer fluid and stiffness of flexible hosing connected to the adsorber bed, show significant contribution in the adsorbate uptake mass measurements. To de-convolute these undesirable effects, a two-step mass measurement is performed to precisely measure the adsorbate uptake rate. To verify the developed method, the equilibrium water uptakes of AQSOA FAM-Z02 are measured and compared against the available data in the literature measured by a thermogravimetric analysis. Next, the water uptake of AQSOA FAM-Z02 is measured for different cycle times, followed by calculation of specific cooling power (SCP) and coefficient of performance (COP). Results show that high heat transfer surface area and small fin spacing are the main specifications of a well-designed adsorber bed for ACS applications. As a result of using AQSOA FAM-Z02 and a well-designed adsorber bed, a SCP of 112.9 W/kg and a COP of 0.34 are achieved at cycle time of 10 min.

1. Introduction

Air conditioning and refrigeration (A/C-R) systems are responsible for using about 30% of the total worldwide energy produced [1] and the number of A/C-R units is expected to reach 78.8 million units by 2015. The Supplemental Federate Test Procedure (SFTP) for emission tests of A/C systems (SC03) in vehicles with gross weight of under 2608 kg showed that A/C systems contributed to 37% of the total tail-pipe emissions [2]. Furthermore, about 70% of the total fuel energy released in an internal combustion engine (ICE) is wasted as a high temperature heat that is dissipated through the engine coolant and exhaust gas [3]. Waste heat-driven adsorption cooling systems (ACS) are potential energy efficient replacements for vapor compression refrigeration cycles (VCRCs) where low-grade thermal energy is available. ACS can use the waste heat of an ICE to provide cooling in vehicles and drastically reduce the fuel consumption and carbon footprint of vehicles.

A waste heat-driven ACS uses an adsorbate, such as water or methanol, that is adsorbed and desorbed from the surface of a solid adsorbent, such as zeolite, silica gel, or activated carbon. Most of these materials are non-toxic, non-corrosive, and inexpensive [4], making ACS a safe and environmentally friendly technology. ACS operate quietly and are easy to maintain because valves are their only moving parts [5]. However, current ACS are limited in their usefulness for commercial vehicle applications, specifically light-duty vehicles, because of their bulkiness and heavy weight. The main challenges facing this technology are low coefficient of performance (COP = cooling energy / input energy) and low specific cooling

* Corresponding author. Tel.: +1 (778) 782 8538; fax: +1 (778) 782 7514.
E-mail address: mbahrami@sfu.ca (M. Bahrami).
[1]These authors have been contributed equally to the work as the first author.

http://dx.doi.org/10.1016/j.applthermaleng.2015.12.060
1359-4311/

power (SCP = cooling energy / (adsorbent mass × cycle time)) that originate from the low thermal conductivity of adsorbent particles (~0.1 to 0.4 W/mK) [6–8] and the low mass diffusivity of adsorbent-adsorbate pairs (~10^{-8} to 10^{-14} m^2/s) [7,9].

To overcome these limitations, different composite adsorbent materials with high thermal conductivity and high adsorbate uptake have been developed such as the ones reported in Refs. [10–14]. AQSOA FAM-Z02 is one of these synthetic materials developed for A/C applications by Mitsubishi Chemical Ltd. [15]. FAM-Z02 showed high durability of 60,000 cycles with no reduction in its uptake capacity and low desorption temperature of 75–95 °C [15], making it a good candidate for ACS applications. However, its thermal conductivity is 0.117 W/mK [16]. Thermogravimetric analysis (TGA) is a well-known technique for measuring the adsorbate uptake of an adsorbent material. In a TGA, mass changes of few milligrams of an adsorbent are measured during adsorption or desorption under a controlled temperature and pressure. The water vapor sorption isotherms of FAM-Z02 measured by a TGA can be found in Refs. [17–20]. The nominal adsorption and desorption temperatures of a waste heat-driven FAM-Z02 ACS reported in the open literature were 30 °C and 90 °C. TGA measurements showed that the equilibrium water uptakes of FAM-Z02 at 30 °C and 90 °C were 0.33 and 0.023 kg/kg with the water vapor source temperature maintained constant at 20 °C [19]. Therefore, the equilibrium water uptake difference of FAM-Z02 under these operating conditions was 0.307 kg/kg. In a real application, however, adsorption and desorption occur under large pressure jumps and non-isothermal conditions, making the operating conditions far from the ideal found in a TGA.

Adsorbate uptake capability of an adsorbent material packed in an adsorber bed may be further reduced by the adsorber bed design, interparticle mass transfer resistance, and pressure drop within the adsorber bed, as well as effects from other components of the ACS, e.g. condenser and evaporator. A metallic wire mesh or perforated sheet is necessary for holding loose adsorbent grains inside the adsorber bed, which contributes to the pressure drop and mass transfer resistance. More importantly, ACS is a dynamic system and, as a result of adsorption and desorption within short cycle times (less than 30 min), the adsorbate uptake of an adsorbent material does not reach the equilibrium value measured by a TGA. Due to these geometrical and operational constrains, the adsorbate uptake capability of an adsorbent material reduces in the short periods of adsorption and desorption processes. To quantify these effects and measure the adsorbate uptake rate of adsorbent materials in conditions close to reality than in a TGA, a variety of experiments have been designed, as summarized in Table 1.

The main goal of these studies, tabulated in Table 1, was to find the effects of large-scale masses (>1 mg) of different adsorbent materials with different grain sizes and number of adsorbent layers on their in-situ adsorbate uptake rate. Riffel et al. [30], Dawoud [37], Gordeeva et al. [38] and Santamaria et al. [39] also studied the effects of different adsorber bed designs on the adsorbate uptake rate of adsorbent materials. Riffel et al. [30] measured the water uptake rate of silica gel and zeolite packed in a finned tube heat exchanger for adsorption times of less than 3 min. They have mentioned that the scale had to be calibrated for each set of experiments because of the flexible tubes and different heat exchangers. However, they had not noted the effects of the density change of the heat transfer fluid during adsorption and desorption on the adsorber bed mass measurements. Dawoud [37] measured the water uptake rate of FAM-Z02 indirectly from the performance analysis of an adsorption heat pump. Using this method can be misleading because of the thermal masses of condenser and evaporator. For example, the thermal mass of an evaporator delays the heat transfer from the chilled water to the adsorbate and calculating the adsorbate uptake of an adsorbent material from the chilled water cooling power results in underestimating the water uptake. To minimize such errors, therefore, in-situ adsorbate uptake rate measurements are preferred. Santamaria et al. [39] calculated the performance of an ACS by measuring the water uptake of FAM-Z02 with 72-90 g mass. Their measurements showed 6–8 times higher values than what they found in their large-scale tests because of mass transfer resistances between particles and the metal mesh wrapped around the adsorber bed, and the designs of the condenser and evaporator of the ACS [39].

Based on the literature review, one can conclude that large-scale adsorbate uptake rate measurements for ACS applications lead to more realistic data than those measured by a TGA, but new parameters affect the measurements and, in some cases, they result in underestimating the adsorbate uptake rate. In this study, we tried to resolve some of these problems, namely, density change of heat transfer fluid and stiffness change of flexible hosing connected to the adsorber bed. The equilibrium water uptake of FAM-Z02 packed in two different adsorber beds is measured in-situ and compared against the TGA data under the adsorption and desorption temperatures of 30 °C and 90 °C, respectively, and the water vapor supplied at 20 °C. The effects of different cycle times on the water uptake rate of FAM-Z02 are also studied. The significance of heat transfer fluid density change and flexible hosing stiffness variations are investigated and, finally, the maximum achievable SCP and COP by using the adsorber beds are calculated.

2. Experimental testbed

To measure the mass exchange of an adsorbent packed in an adsorber bed under adsorption or desorption, an experimental test setup was designed and built as shown in Fig. 1. The adsorber bed was placed on a scale (Setra, Supper II) with ±1 g accuracy and connected to cooling and heating fluid temperature control systems, TCS_{CF} and TCS_{HF}, for intermittent adsorption and desorption. A water source at a constant temperature, shown in Fig. 1, was connected to the adsorber bed using a vacuum rated flexible hose. This water source served as an evaporator and a condenser during adsorption and desorption, respectively.

To test the effects of different adsorber bed designs, two heat exchangers with different geometries (No. 1 in Fig. 2a and 2b) were connected to the evaporator/condenser container (No. 3 in Fig. 2a and 2b). The first heat exchanger (called Design I) was built based on the results of Sharafian et al. [44] and was placed inside a vacuum chamber, as shown in Fig. 2a. The second adsorber bed (called Design II), which was an engine oil cooler manufactured by Hayden Automotive (model #1268), was placed in a custom-built vacuum chamber, as shown in Fig. 2b. The heat exchangers in Designs I and II had the same mass. However, the fin spacing and heat transfer surface area of heat exchangers in Designs I and II were 6.47 mm and 0.235 m^2, and 2.34 mm and 2.8 m^2, respectively. To measure the temperature and pressure of the adsorber beds and evaporator/condenser container, thermocouples type T (Omega, model #5SRTC-TT-T-36-36) with accuracy of 0.75% of reading in degree Celsius, and two pressure transducers (Omega, model #PX309-005AI) with 0–34.5 kPa absolute pressure range and ±0.4 kPa accuracy were installed. A positive displacement flow meter (FLOMEC, Model # OM015S001-222) with accuracy of 0.5% of reading in L/min was installed on the adsorber bed to measure the heating and cooling fluid flow rates. Table 2 shows further details on the adsorber bed geometries and operating conditions. It can be seen in Table 2 that the amount of adsorbent material inside the adsorber bed of Design II is more than that of Design I. To supply enough water vapor during adsorption process, two evaporators of the same type were connected to the adsorber bed of Design II, as shown in Fig. 2b.

The adsorber bed, packed with the FAM-Z02, was heated using a 90 °C heating fluid and simultaneously evacuated for 8 hours to be completely dried out. The adsorber bed was then placed on the scale and connected to the evaporator, TCS_{HF}, and TCS_{CF}. For an adsorption process, TCS_{CF} circulated a 30 °C cooling fluid to the adsorber

Table 1
In-situ adsorbate uptake rate measurements of different adsorbent materials in a large-scale test bed.

Ref.	Adsorbent-adsorbate pair	Adsorbent mass	Purpose
Dawoud and Aristov [21]	Mesoporous silica gel-water Alumina-water Silica gel + $CaCl_2$ (SWS-1L)-water Alumina + $CaCl_2$ (SWS-1A)-water	3 g	Measuring the kinetics of water sorption of loose adsorbent grains under real ACS operating conditions
Aristov et al. [22,23]	Silica gel + $CaCl_2$ (SWS-1L)-water	0.022–0.025 g	Effects of grain size (0.7-2.8 mm) and temperature (33-69 °C) on the kinetics of water sorption of SWS-1L under real ACS operating conditions
Dawoud [17]	FAM-Z02-water	0.150 g	Effects of grain size (0.7-2.6 mm) on water sorption rate of FAM-Z02 under real ACS operating conditions
Dawoud et al. [24]	Consolidated zeolite-water	3 g	Measuring the kinetics of water sorption of consolidated zeolite layer with 0.7 mm thickness on an aluminum substrate under real ACS operating conditions
Glaznev and Aristov [25–27] Glaznev et al. [16]	Silica gel + $CaCl_2$ (SWS-1L)-water RD silica gel-water FAM-Z02-water	0.420–0.425 g	Effects of residual air on water sorption rate of adsorbents under real ACS operating conditions
Storch et al. [28]	Zeolite 13X-water	180 g	Effects of 3500 adsorption/desorption cycles on the equilibrium water uptake of zeolite 13X
Schnabel et al. [29]	Coated zeolite A-water Coated zeolite X-water	0.170 g 1.030 g	Measuring water uptake rate of zeolite coated directly on a metallic substrate
Riffel et al. [30]	Silica gel-water Zeolite water	1.051 kg 1.093 kg	Measuring water uptake rate of two different adsorbent materials packed in a finned tube heat exchanger under real ACS operating conditions
Solmuş et al. [31]	Natural zeolite-water	1.667 g	Measuring equilibrium water uptake of zeolite packed in an adsorber bed
Ovoshchnikov et al. [32]	Silica gel + $CaCl_2$ (SWS-1L)-water	-	Measuring water uptake rate of SWS-1L to find different water diffusion mechanism inside SWS-1L
Askalany et al. [33]	Activated carbon-R134a	-	Measuring equilibrium R134a uptake of granular activated carbon
Aristov et al. [34] Aristov [35] Chakraborty et al. [36]	RD silica gel-water	-	Effects of adsorbent grain size and number of adsorbent layers on its water uptake rate under large temperature jumps
Dawoud [37]	FAM-Z02-water	204 g 1.5-2.53 kg	Calculating the kinetics of water uptake of FAM-Z02 indirectly by using the performance analysis of an adsorption heat pump
Gordeeva et al. [38]	LiBr + silica gel-ethanol	0.300 g 56-76 g	Measuring in-situ ethanol uptake rate of loose LiBr + silica gel grains packed in finned tube heat exchangers with different length/height ratios
Santamaria et al. [39]	FAM-Z02-water	72-90 g	Effect of heat exchanger geometry, adsorbent grain size and heat transfer fluid flow rate on in-situ water uptake rate measurement of FAM-Z02
Frazzica et al. [40]	SAPO 34 + bentonite clay + carbon fiber-water	0.26-0.85 g	Measuring the water uptake rate of the composite adsorbent coated on a metallic plate with different thicknesses
Sapienza et al. [41]	SAPO 34-water	4.49–33.13 g	Effects of adsorbent grain size and number of adsorbent layers on in-situ water uptake rate measurement of SAPO 34 under real ACS operating conditions
Gordeeva and Aristov [42]	Activated carbon ACM-35.4-methanol	0.5 g	Effects of 0.8-4.0 mm adsorbents and number of adsorbent layers on water uptake rate of activated carbon ACM-35.4
Freni et al. [43]	Coated SAPO 34-water	84 g	Measuring in-situ water uptake rate of SAPO 34 with 0.1 mm thickness coated on an aluminum heat exchanger under real ACS operating conditions

bed and once the valve between the adsorber bed and the evaporator was opened the FAM-Z02 adsorbed the water vapor from the evaporator. This adsorption caused the adsorber bed mass to increase over time. For a desorption process, the adsorber bed was heated up with a 90 °C heating fluid and the adsorber bed mass reduced due to desorption of water.

3. Data analysis

The performance of the adsorber beds is evaluated by calculating the COP and SCP of the ACS. Eq. (1) gives the ideal evaporation cooling energy, calculated based on the in-situ water uptake rate measurements of FAM-Z02:

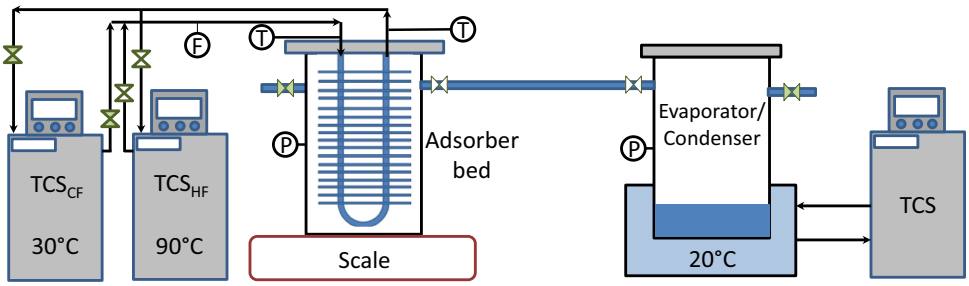

Fig. 1. Schematic of the experimental test setup.

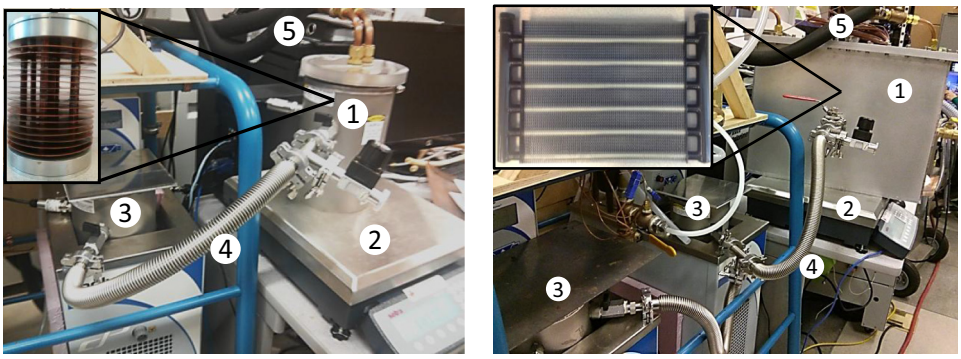

Fig. 2. Details of the experimental setup for (a) Design I and (b) Design II. 1: adsorber bed, 2: scale, 3: evaporator/condenser, 4: flexible hose, and 5: heating/cooling fluid ports.

$$Q_{evap,ideal}(J) = \Delta\omega_{adsorption} m_{adsorbent} h_{fg} \quad (1)$$

where $\Delta\omega_{adsorption}$ is equal to $\Delta m_{adsrobate\ uptake}/m_{adsorbent}$, i.e. the amount of water adsorbed during an adsorption process over the mass of dry adsorbent, and h_{fg} is the enthalpy of evaporation of water at the evaporator temperature. In this study, the ideal evaporation cooling energy refers to an evaporator with the effectiveness of one and thermal mass of zero in which there is no temperature drop between the refrigerant and the chilled water circulated inside the evaporator. This assumption is in agreement with the data measured using a TGA such as the data reported in Ref. [17]. The total heat transfer to the adsorbent material during a desorption process is:

$$Q_{total\ heating}(J) = \int_{desorption} \dot{m}_{hf} c_{p,hf} (T_{hf,i} - T_{hf,o}) dt \quad (2)$$

where $\dot{m}_{hf}$ is the heating fluid mass flow rate and $T_{hf,i}$ -$T_{hf,o}$ is the temperature difference between the inlet and outlet of the adsorber bed. Using Eqs. (1) and (2), the ideal COP and SCP of the ACS can be calculated:

Table 2
Specifications of adsorber beds and operating conditions.

Parameter	Design I	Design II
Working pairs	AQSOA FAM-Z02/water	
Adsorbent particles diameter (m)	0.002	
Mass of adsorbent (kg)	0.62	1.50
Metal mass of adsorber bed (kg)	2.80	2.87
Adsorber bed heat transfer surface area, A_{bed}, (m^2)	0.235	2.80
Fin spacing (mm)	6.47 (3.5 fins per inch)	2.34 (10 fins per inch)
Fin dimensions	12.7 cm (5") diameter	43.18 × 30.48 cm (17" × 12")
Heating fluid mass flow rate to adsorber bed (kg/s)	0.058 (4.1 L/min of silicone oil)	
Cooling fluid mass flow rate to adsorber bed (kg/s)	0.062 (4.1 L/min of silicone oil)	
Heat capacity of silicone oil (kJ/kgK)	1.8	
Heating fluid inlet temperature (°C)	90	
Cooling fluid inlet temperature (°C)	30	
Evaporation/ condensation temperature (°C)	20	

$$COP_{ideal} = \frac{Q_{evap,ideal}}{Q_{total\ heating}} \quad (3)$$

$$SCP_{ideal}(W/kg) = \frac{Q_{evap,ideal}}{m_{adsobent}\,\tau_{cycle}} \quad (4)$$

where τ_{cycle} in Eq. (4) is the cycle time.

4. Results and discussion

4.1. Effect of changes in density of heat transfer fluid and stiffness of hosing on in-situ mass measurements

Fig. 3 shows the variations in the heating and cooling fluid inlet and outlet temperatures, and the mass changes of the adsorber bed in Design II during adsorption and desorption at cycle time of 60 min. It can be seen in Fig. 3 that by cooling the adsorber bed in Design II, adsorption process starts and mass of adsorber bed increases. At the end of adsorption process, the mass of the adsorber bed reaches its maximum value. By heating the adsorber bed, the adsorbate is desorbed from the FAM-Z02 and flows to the condenser, and as a result, the mass of the adsorber bed starts reducing, as shown in Fig. 3b.

The heat transfer fluid used for heating and cooling of the adsorber beds was silicone oil (Julabo, Thermal P60), which had a density change from 909 kg/m^3 at 30 °C to 854 kg/m^3 at 90 °C. Further, the stiffness of the hosing connected to the adsorber beds changed during heating and cooling processes and affected the mass measurements. To eliminate these undesirable changes in the adsorber bed mass measurements, the adsorber beds were disconnected from the evaporator/condenser container, and heating and cooling processes were performed to measure the adsorber bed mass change caused only by the variations of heat transfer fluid density and the stiffness of the hosing. Fig. 3b indicates that these variations can have significant effects on the adsorber bed mass measurement and, consequently, the water uptake rate calculations and should thus be de-convoluted from the measured data.

Fig. 4 shows the variation of evaporator/condenser pressure, $P_{evap/cond}$, for Designs I and II under a cycle time of 60 min. The red line in Fig. 4 shows the saturation pressure of water at 20 °C. It can be seen in Fig. 4 that during the adsorption process, the adsorber beds in Designs I and II create suction, and $P_{evap/cond}$ reduces. This reduction in the evaporator pressure causes water to start evaporating inside the evaporator. Fig. 4 also indicates that $P_{evap/cond}$ is lower when the evaporator is connected to the adsorber bed in Design II than when it is connected to the adsorber bed in Design I, because of

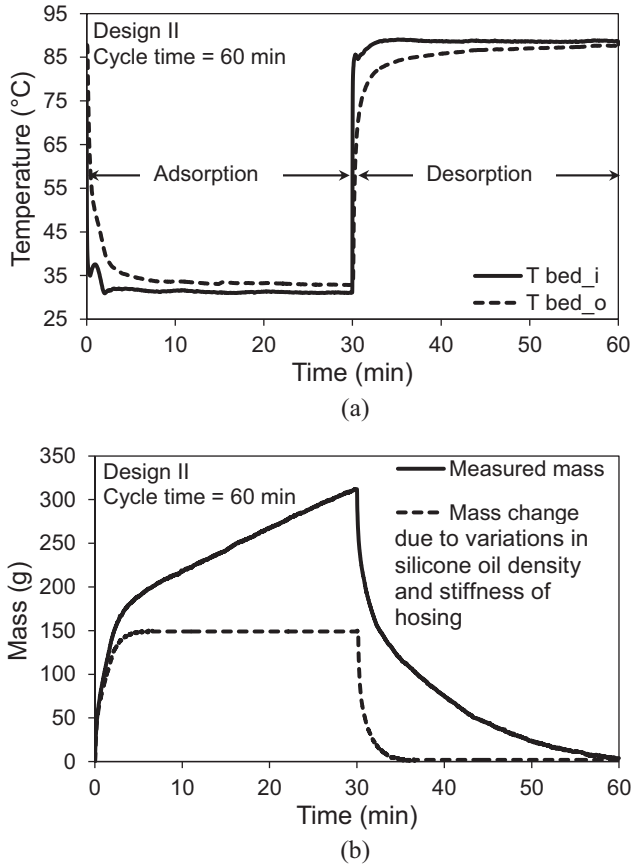

Fig. 3. (a) Heating and cooling fluid inlet and outlet temperatures and (b) mass changes of adsorber bed in Design II and mass change due to variations in silicone oil density and stiffness of hosing during adsorption and desorption under cycle time of 60 min.

higher suction created by the adsorber bed in Design II. Higher suction by the adsorber bed in Design II causes more water evaporation and, as a result, the FAM-Z02 adsorbs more water vapor within a constant adsorption time. By heating the adsorber beds in the desorption process, water is desorbed from the FAM-Z02 and pressures of the adsorber beds increase. Due to the pressure gradient between the adsorber bed and the condenser container, water vapor is pushed from the adsorber beds to the condenser.

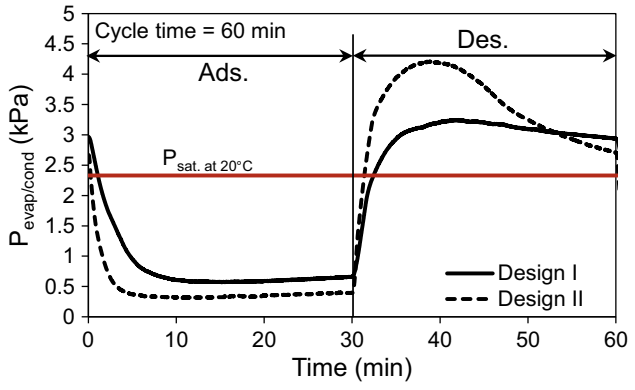

Fig. 4. Variations in $P_{evap/cond}$ due to the different adsorber beds in Designs I and II during the adsorption and desorption processes. The red line demarcates the saturation pressure of water at 20 °C.

4.2. Effects of adsorber bed design on the equilibrium water uptake of FAM-Z02

To compare the equilibrium data collected using our experimental setup and the TGA data reported in Ref. [19], two adsorption and desorption isotherm tests were run under the operating conditions summarized in Table 2. To run the equilibrium adsorption test, the dried FAM-Z02 packed in the adsorber beds of Designs I and II was exposed to the water vapor provided by the evaporator at a constant temperature of 20 °C. As shown in Fig. 5a, the FAM-Z02 adsorbs the water vapor and the adsorber bed mass increases until it reaches a constant value of 30% kg/kg. It can be seen in Fig. 5a that the mass of the adsorber bed in Design II increases faster than that in Design I. This is because of the higher heat transfer surface area and faster removal of the heat of adsorption from the adsorber bed. At the adsorption time of 240 min, the equilibrium water uptakes of both adsorber beds reach the same value. Fig. 5a also indicates that the equilibrium water uptakes measured using Designs I and II are 3% (= 33–30%) less than that measured by the TGA because of mass resistances inside the adsorber beds which make the operating condition different from ideal condition.

Fig. 5b shows the desorption curves for Designs I and II under the operating conditions tabulated in Table 2. Fig. 5b demonstrates that the adsorber bed of Design II results in faster water desorption from the FAM-Z02 due to the higher heat transfer rate. Also, at the end of the desorption process the equilibrium water uptake of FAM-Z02 in Design II is 1.6% kg/kg less than that in Design I. The equilibrium water uptakes at the end of the desorption tests of Designs I and II are 3.8% and 2.2% kg/kg more than that of the TGA measurement. Finally, by comparing the running times of

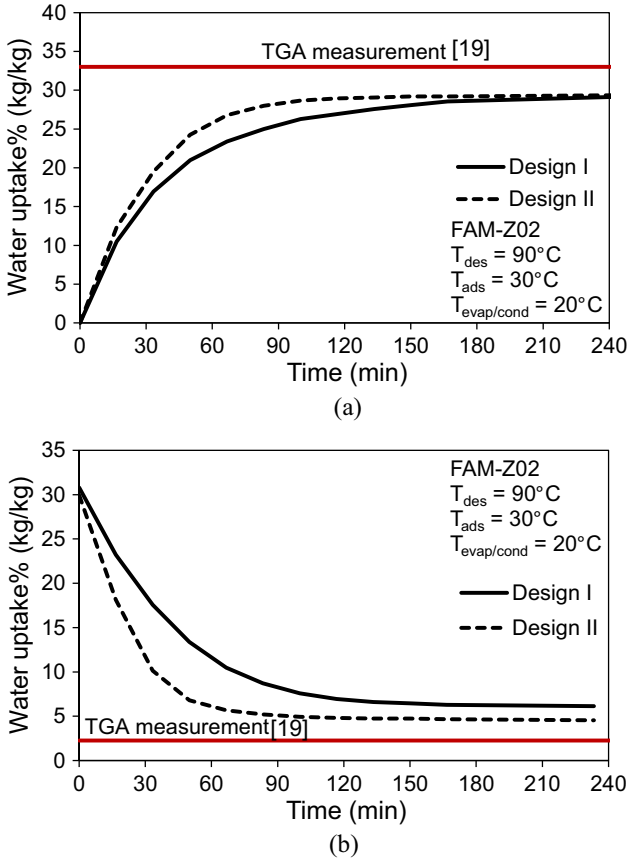

Fig. 5. (a) Adsorption and (b) desorption isotherms measured by using Designs I and II, and compared against the TGA data measurements reported in Ref. [19].

adsorption and desorption processes in Design II, one can conclude that the desorption time (120 min) is almost two times shorter than the adsorption time (240 min) under the defined operating conditions. The slope of changes in the mass measured over time is the criterion for reaching to equilibrium under adsorption or desorption. This slope can be set by the user. We set the changes in the mass measured over time to be less than 0.033 g/min which is equal to 2 g changes in the mass measured over 60 min.

4.3. Effects of adsorber designs on the performance of an ACS

The FAM-Z02 water uptake differences, $\Delta\omega$, between two continuous adsorption and desorption processes were measured in-situ under different cycle times, as shown in Fig. 6a. It can be seen in Fig. 6a that the adsorber bed in Design II provides higher $\Delta\omega$ than that in Design I for a constant cycle time. For example, under the cycle time of 60 min, the adsorber beds in Designs I and II provide $\Delta\omega$ of 3.5% and 10.8% kg/kg, respectively (three times higher uptake for Design II). The main reasons for this significant difference between the $\Delta\omega$ of Designs I and II are the high heat transfer surface area and small fin spacing of the adsorber bed in Design II. These features help the FAM-Z02 adsorb more water vapor during adsorption by more quickly removing the heat of adsorption. Using the measured $\Delta\omega$, the SCP_{ideal} and COP_{ideal} of Designs I and II can be calculated.

Fig. 6b shows that the SCP_{ideal} of Design I varies between 23.8 and 29.3 W/kg for cycle times of 60–180 min. In contrast, the SCP_{ideal} of Design II decreases from 112.9 to 63.2 W/kg by increasing the cycle time from 10 to 120 min. Fig. 6c displays that the COP_{ideal} of Design I increases from 0.22 to 0.40 as cycle time is increased from 60 to 180 minutes while the COP_{ideal} of Design II increases from 0.34 to 0.67 as the cycle time is increased from 10 to 120 min. Comparing the SCP_{ideal} and COP_{ideal} of Designs I and II, as shown in Fig. 6, indicates that high heat transfer surface area and small fin spacing are two key features of a well-designed adsorber bed for ACS applications and having a proper adsorbent material, such as FAM-Z02, is not necessarily sufficient to reach high ACS performance.

5. Conclusion

The effects of different adsorber bed designs on the performance of an ACS were studied by in-situ water uptake rate measurements of FAM-Z02. The results of a comprehensive literature review showed that large-scale adsorbate uptake rate mass measurements could result in closer performance prediction of an ACS than the adsorbate uptake rate measurements from a TGA. However, other issues affected the mass measurements, such as changes in the density of the heat transfer fluid and variations in the stiffness of the flexible hosing connected to the adsorber beds. In this study, a systematic procedure was introduced to de-convolute these parameters from the in-situ mass measurements to get a precise adsorbate uptake rate and uptake difference measurements. The performance of an ACS was studied under different cycle times and the results showed that high heat transfer surface area and small fin spacing were key features of a good adsorber bed design for ACS applications. Finally, the results indicated that a combination of high quality adsorbent (FAM-Z02) and a well-designed adsorber bed could produce a SCP_{ideal} of 112.9 W/kg and a COP_{ideal} 0.34 at cycle time of 10 min.

Acknowledgements

The authors gratefully acknowledge the financial support of the Natural Sciences and Engineering Research Council of Canada (NSERC) through the Automotive Partnership Canada Grant No. APCPJ 401826-10.

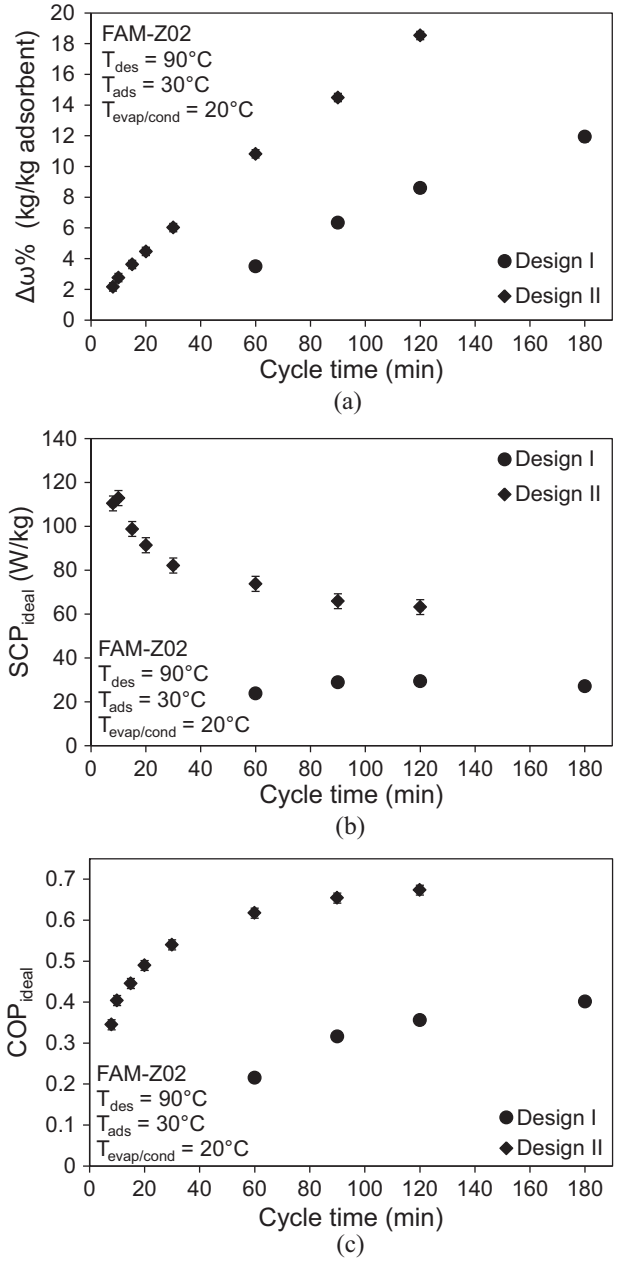

Fig. 6. (a) FAM-Z02 water uptake difference between adsorption and desorption processes, (b) SCP_{ideal} and (c) COP_{ideal} in Designs I and II vs. different cycle times.

Nomenclature

ACS	Adsorption cooling system
A/C	Air conditioning
A/C-R	Air conditioning and refrigeration
c_p	Heat capacity at constant pressure (*J/kg.K*)
COP	Coefficient of performance
h_{fg}	Enthalpy of evaporation (*J/kg*)
ICE	Internal combustion engine
m	Mass (*kg*)
$\dot{m}$	Mass flow rate (*kg/s*)
P	Pressure (*kPa*)
Q_{total}	Total heat transfer (*J*)
SCP	Specific cooling power (*W/kg dry adsorbent*)
SFTP	Supplemental federal test procedure
ω	Adsorbate uptake (*kg/kg dry adsorbent*)

T	Temperature (K)
t	Time (s)
τ_{cycle}	Cycle time (s)
TCS	Temperature control system
TGA	Thermogravimetric analysis
VCRC	Vapor compression refrigeration cycle

Subscripts

adsorbate	Adsorbate
adsorbent	Adsorbent particles
cf	Cooling fluid
cond	Condenser
evap	Evaporator
hf	Heating fluid
i	In
o	Out

References

[1] L.O.S. Buzelin, S.C. Amico, J.V.C. Vargas, J.A.R. Parise, Experimental development of an intelligent refrigeration system, Int. J. Refrig. 28 (2005) 165–175, doi:10.1016/j.ijrefrig.2004.08.013.

[2] R. Farrington, J. Rugh Impact of vehicle air-conditioning on fuel economy, tailpipe emissions, and electric vehicle range. Proceeding Earth Technol. Forum, Washington, D.C.: 2000.

[3] M. Suzuki, Application of adsorption cooling systems to automobiles, Heat Recov. Syst. CHP 13 (1993) 335–340.

[4] M.O. Abdullah, I.A.W. Tan, L.S. Lim, Automobile adsorption air-conditioning system using oil palm biomass-based activated carbon: a review, Renew. Sustain. Energy Rev. 15 (2011) 2061–2072, doi:10.1016/j.rser.2011.01.012.

[5] H. Demir, M. Mobedi, S. Ülkü, A review on adsorption heat pump: problems and solutions, Renew. Sustain. Energy Rev. 12 (2008) 2381–2403, doi:10.1016/j.rser.2007.06.005.

[6] F. Poyelle, J.J. Guilleminot, F. Meunier, Experimental tests and predictive model of an adsorptive air conditioning unit, Ind. Eng. Chem. Res. 38 (1999) 298–309, doi:10.1021/ie9802008.

[7] Z. Tamainot-Telto, R.E. Critoph, Monolithic carbon for sorption refrigeration and heat pump applications, Appl. Therm. Eng. 21 (2001) 37–52, doi:10.1016/S1359-4311(00)00030-2.

[8] A. Freni, M.M. Tokarev, G. Restuccia, A.G. Okunev, Y.I. Aristov, Thermal conductivity of selective water sorbents under the working conditions of a sorption chiller, Appl. Therm. Eng. 22 (2002) 1631–1642, doi:10.1016/S1359-4311(02)00076-5.

[9] A. Sharafian, M. Bahrami, Adsorbate uptake and mass diffusivity of working pairs in adsorption cooling systems, Int. J. Heat Mass Transf. 59 (2013) 262–271, doi:10.1016/j.ijheatmasstransfer.2012.12.019.

[10] L.W. Wang, Z. Tamainot-Telto, R. Thorpe, R.E. Critoph, S.J. Metcalf, R.Z. Wang, Study of thermal conductivity, permeability, and adsorption performance of consolidated composite activated carbon adsorbent for refrigeration, Renew. Energy 36 (2011) 2062–2066, doi:10.1016/j.renene.2011.01.005.

[11] A.A. Askalany, M. Salem, I.M. Ismael, A.H.H. Ali, M.G. Morsy, B.B. Saha, An overview on adsorption pairs for cooling, Renew. Sustain. Energy Rev. 19 (2013) 565–572, doi:10.1016/j.rser.2012.11.037.

[12] Y. Aristov, Concept of adsorbent optimal for adsorptive cooling/heating, Appl. Therm. Eng. 72 (2014) 166–175, doi:10.1016/j.applthermaleng.2014.04.077.

[13] K.C. Chan, C.Y.H. Chao, C.L. Wu, Measurement of properties and performance prediction of the new MWCNT-embedded zeolite 13X/CaCl2 composite adsorbents, Int. J. Heat Mass Transf. 89 (2015) 308–319 <http://dx.doi.org/10.1016/j.ijheatmasstransfer.2015.05.063>.

[14] U. Wittstadt, G. Füldner, O. Andersen, R. Herrmann, F. Schmidt, A new adsorbent composite material based on metal fiber technology and its application in adsorption heat exchangers, Energies 8 (2015) 8431–8446, doi:10.3390/en8088431.

[15] S.S. Himooka, K.O. Shima, The evaluation of direct cooling and heating desiccant device coated with FAM, J. Chem. Eng. Japan 40 (2007) 1330–1334.

[16] I. Glaznev, D. Ovoshchnikov, Y.I. Aristov, Effect of residual gas on water adsorption dynamics under typical conditions of an adsorption chiller, Heat Transf. Eng. 31 (2010) 924–930, doi:10.1080/01457631003604335.

[17] B. Dawoud, On the effect of grain size on the kinetics of water vapor adsorption and desorption into/from loose pellets of FAM-Z02 under a typical operating condition of adsorption heat pumps, J. Chem. Eng. Japan 40 (2007) 1298–1306, doi:10.1252/jcej.07WE163.

[18] S.K. Henninger, F.P. Schmidt, H.M. Henning, Water adsorption characteristics of novel materials for heat transformation applications, Appl. Therm. Eng. 30 (2010) 1692–1702, doi:10.1016/j.applthermaleng.2010.03.028.

[19] K. Okamoto, M. Teduka, T. Nakano, S. Kubokawa, H. Kakiuchi The development of AQSOA water vapor adsorbent and AQSOA coated heat exchanger. Int. Symp. Innov. Mater. Process. Energy Syst., Singapor: 2010.

[20] M.J. Goldsworthy, Measurements of water vapour sorption isotherms for RD silica gel, AQSOA-Z01, AQSOA-Z02, AQSOA-Z05 and CECA zeolite 3A, Microporous Mesoporous Mater. 196 (2014) 59–67, doi:10.1016/j.micromeso.2014.04.046.

[21] B. Dawoud, Y.I. Aristov, Experimental study on the kinetics of water vapor sorption on selective water sorbents, silica gel and alumina under typical operating conditions of sorption heat pumps, Int. J. Heat Mass Transf. 46 (2003) 273–281, doi:10.1016/S0017-9310(02)00288-0.

[22] Y.I. Aristov, I.S. Glaznev, A. Freni, G. Restuccia, Kinetics of water sorption on SWS-1L (calcium chloride confined to mesoporous silica gel): influence of grain size and temperature, Chem. Eng. Sci. 61 (2006) 1453–1458, doi:10.1016/j.ces.2005.08.033.

[23] Y.I. Aristov, B. Dawoud, I.S. Glaznev, A. Elyas, A new methodology of studying the dynamics of water sorption/desorption under real operating conditions of adsorption heat pumps: experiment, Int. J. Heat Mass Transf. 51 (2008) 4966–4972, doi:10.1016/j.ijheatmasstransfer.2007.10.042.

[24] B. Dawoud, U. Vedder, E.-H. Amer, S. Dunne, Non-isothermal adsorption kinetics of water vapour into a consolidated zeolite layer, Int. J. Heat Mass Transf. 50 (2007) 2190–2199, doi:10.1016/j.ijheatmasstransfer.2006.10.052.

[25] I.S. Glaznev, Y.I. Aristov, Kinetics of water adsorption on loose grains of SWS-1L under isobaric stages of adsorption heat pumps: the effect of residual air, Int. J. Heat Mass Transf. 51 (2008) 5823–5827, doi:10.1016/j.ijheatmasstransfer.2008.04.061.

[26] B.N. Okunev, A.P. Gromov, V.L. Zelenko, I.S. Glaznev, D.S. Ovoshchnikov, L.I. Heifets, et al., Effect of residual gas on the dynamics of water adsorption under isobaric stages of adsorption heat pumps: mathematical modelling, Int. J. Heat Mass Transf. 53 (2010) 1283–1289, doi:10.1016/j.ijheatmasstransfer.2009.12.040.

[27] I.S. Glaznev, Y.I. Aristov, The effect of cycle boundary conditions and adsorbent grain size on the water sorption dynamics in adsorption chillers, Int. J. Heat Mass Transf. 53 (2010) 1893–1898, doi:10.1016/j.ijheatmasstransfer.2009.12.069.

[28] G. Storch, G. Reichenauer, F. Scheffler, A. Hauer, Hydrothermal stability of pelletized zeolite 13X for energy storage applications, Adsorption 14 (2008) 275–281, doi:10.1007/s10450-007-9092-7.

[29] L. Schnabel, M. Tatlier, F. Schmidt, A. Erdem-Şenatalar, Adsorption kinetics of zeolite coatings directly crystallized on metal supports for heat pump applications (adsorption kinetics of zeolite coatings), Appl. Therm. Eng. 30 (2010) 1409–1416, doi:10.1016/j.applthermaleng.2010.02.030.

[30] D.B. Riffel, U. Wittstadt, F.P. Schmidt, T. Núñez, F.A. Belo, A.P.F. Leite, et al., Transient modeling of an adsorber using finned-tube heat exchanger, Int. J. Heat Mass Transf. 53 (2010) 1473–1482, doi:10.1016/j.ijheatmasstransfer.2009.12.001.

[31] İ. Solmuş, C. Yamalı, B. Kaftanoğlu, D. Baker, A. Çağlar, Adsorption properties of a natural zeolite–water pair for use in adsorption cooling cycles, Appl. Energy 87 (2010) 2062–2067, doi:10.1016/j.apenergy.2009.11.027.

[32] D.S. Ovoshchnikov, I.S. Glaznev, Y.I. Aristov, Water sorption by the calcium chloride/silica gel composite: the accelerating effect of the salt solution present in the pores, Kinet. Catal. 52 (2011) 620–628, doi:10.1134/S0023158411040124.

[33] A.A. Askalany, M. Salem, I.M. Ismail, A.H.H. Ali, M.G. Morsy, Experimental study on adsorption–desorption characteristics of granular activated carbon/R134a pair, Int. J. Refrig. 35 (2012) 494–498, doi:10.1016/j.ijrefrig.2011.04.002.

[34] Y.I. Aristov, I.S. Glaznev, I.S. Girnik, Optimization of adsorption dynamics in adsorptive chillers: loose grains configuration, Energy 46 (2012) 484–492, doi:10.1016/j.energy.2012.08.001.

[35] Y.I. Aristov, Experimental and numerical study of adsorptive chiller dynamics: loose grains configuration, Appl. Therm. Eng. 61 (2013) 841–847, doi:10.1016/j.applthermaleng.2013.04.051.

[36] A. Chakraborty, B. Baran, Y.I. Aristov, Dynamic behaviors of adsorption chiller: effects of the silica gel grain size and layers, Energy 78 (2014) 304–312, doi:10.1016/j.energy.2014.10.015.

[37] B. Dawoud, Water vapor adsorption kinetics on small and full scale zeolite coated adsorbers; A comparison, Appl. Therm. Eng. 50 (2013) 1645–1651, doi:10.1016/j.applthermaleng.2011.07.013.

[38] L. Gordeeva, A. Frazzica, A. Sapienza, Y.I. Aristov, A. Freni, Adsorption cooling utilizing the "LiBr/silica – ethanol" working pair: dynamic optimization of the adsorber/heat exchanger unit, Energy 75 (2014) 390–399, doi:10.1016/j.energy.2014.07.088.

[39] S. Santamaria, A. Sapienza, A. Frazzica, A. Freni, I.S. Girnik, Y.I. Aristov, Water adsorption dynamics on representative pieces of real adsorbers for adsorptive chillers, Appl. Energy 134 (2014) 11–19, doi:10.1016/j.apenergy.2014.07.053.

[40] A. Frazzica, G. Füldner, A. Sapienza, A. Freni, L. Schnabel, Experimental and theoretical analysis of the kinetic performance of an adsorbent coating composition for use in adsorption chillers and heat pumps, Appl. Therm. Eng. 73 (2014) 1020–1029, doi:10.1016/j.applthermaleng.2014.09.004.

[41] A. Sapienza, S. Santamaria, A. Frazzica, A. Freni, Y.I. Aristov, Dynamic study of adsorbers by a new gravimetric version of the Large Temperature Jump method, Appl. Energy 113 (2014) 1244–1251, doi:10.1016/j.apenergy.2013.09.005.

[42] L. Gordeeva, Y.I. Aristov, Dynamic study of methanol adsorption on activated carbon ACM-35.4 for enhancing the specific cooling power of adsorptive chillers, Appl. Energy 117 (2014) 127–133, doi:10.1016/j.apenergy.2013.11.073.

[43] A. Freni, L. Bonaccorsi, L. Calabrese, A. Caprì, A. Frazzica, A. Sapienza, SAPO-34 coated adsorbent heat exchanger for adsorption chillers, Appl. Therm. Eng. 82 (2015) 1–7, doi:10.1016/j.applthermaleng.2015.02.052.

[44] A. Sharafian, C. McCague, M. Bahrami, Impact of fin spacing on temperature distribution in adsorption cooling system for vehicle A/C applications, Int. J. Refrig. 51 (2015) 135–143.